MITSUBISHI ELECTRIC RESEARCH LABORATORIES
http://www.merl.com

Optimal Array Beamforming for Microwave Power Transmission in Complex Environment

Zhang, C.; Wang, B.; Ishimaru, A.; Kuga, Y.

TR2017-032 November 2016

Abstract

Wireless Power Transfer(WPT) is a popular research field in recent years and can be categorized into three approaches: inductive coupling, laser beaming and microwave power transmission(MPT). MPT system operates at the microwave frequency and transfer the energy over more than a few wavelengths. It has its unique advantages of supplying power to non-accessible and mobile receivers. The overall efficiency, which is the ratio between available DC power at receiver and supplied DC power at transmitter, depends on both circuit design and wave propagation. As a comprehensive theory of MPT system is not available, this chapter starts with the study of MPT system from the perspectives of mathematical formulation and the experiment in indoor environment, in Section 1. The preliminary study leads to the conclusion that highly directional wireless transmitter is very useful in the MPT system for achieving high transmission efficiency. For this reason, phased array antennas with beamforming funtionality are usually used to direct the electromagnetic wave towards mobile receivers, and adaptive array algorithms are implemented to enable wireless power focusing in complex environment. Section 3 presents a novel beamforming algorithm, which is proven to give the optimal transmssion efficiency and applies to the abitrarily positioned unequal array based on our problem formulation. To verify this algorithm, Section 4 validates it with numerical electromagnetic simulation in different cases. The numerical comparison in these examples shows that this algorithm gives higher transmission efficiency over other optimal beamforming algrithms discussed in Section 2.

Springer

Optimal Array Beamforming for Microwave Power Transmission in Complex Environment

Ce Zhang, Bingnan Wang, Akira Ishimaru and Yasuo Kuga

Abstract Wireless Power Transfer(WPT) is a popular research field in recent years and can be categorized into three approaches: inductive coupling, laser beaming and microwave power transmission(MPT). MPT system operates at the microwave frequency and transfer the energy over more than a few wavelengths. It has its unique advantages of supplying power to non-accessible and mobile receivers. The overall efficiency, which is the ratio between available DC power at receiver and supplied DC power at transmitter, depends on both circuit design and wave propagation. As a comprehensive theory of MPT system is not available, this chapter starts with the study of MPT system from the perspectives of mathematical formulation and the experiment in indoor environment, in Section 1. The preliminary study leads to the conclusion that highly directional wireless transmitter is very useful in the MPT system for achieving high transmission efficiency. For this reason, phased array antennas with beamforming funtionality are usually used to direct the electromagnetic wave towards mobile receivers, and adaptive array algorithms are implemented to enable wireless power focusing in complex environment. Section 3 presents a novel beamforming algorithm, which is proven to give the optimal transmssion efficiency and applies to the abitrarily positioned unequal array based on our problem formulation. To verify this algorithm, Section 4 validates it with numerical electromagnetic simulation in different cases. The numerical comparison in these examples shows that this algorithm gives higher transmission efficiency over other optimal beamforming algrithms discussed in Section 2.

Ce Zhang, Akira Ishimaru and Yasuo Kuga
University of Washington, Department of Electrical Engineering, Seattle, WA, 98195 e-mail: cezhang2@uw.edu

Bingnan Wang
Mitsubishi Electric Research Lab, 201 Broadway, 8th Floor Cambridge, MA 02139-1955 e-mail: bwang@merl.com

1 Microwave Power Transmission System

Microwave power transmission(MPT) is a promising technology for its capability of suppling energy to receivers over a long range, so it is also called long distance wireless power transmission in [9]. MPT has a variety of applications such as powering ubiquitous sensor nodes at low power level [19], and transferring energy to electrical vehicle [15] [13], unmanned aerial vehicles(UAV)and high altitude platforms(HAPs)at high power level [5] [12]. In addition, MPT has also been proposed and implemented in the very-high-power transmission from the space to earth, which is called "Solar Power Satellites"(SPSs) [10].

The estimation of MPT system efficiency with high accuracy is a challenging task, as there is no theory available for accurately modelling the electromagnetic wave radiation and reception. We start this section with the general formulation of the MPT, which clarifies the efficiencies of different building blocks in MPT system. Then we study the transmission efficiency from different perspectives. If the gain of transmit and receive antenna is known, the quick estimation of transmission efficiency is easy but its accuracy is highly limited. If the channel transfer matrix between the transmit and receive array and impedance matrix of transmit array can be measured with the built-in hardware in the RF system, a more accurate and dynamic transmission efficiency can be found with our proposed model in this section. Following the theoretical study, an experiment has been carried out in the lab environment with clutters such as equipment and furniture. The meausurement data is analyzed with the help of simulation data and gives us an insight into the power loss contribution of the MPT system. The experiment shows that the propagation loss contributes to the most significant percentage of system loss, given the highly efficient wireless power transmitter and receiver.

1.1 Problem Formulation

In the MPT system, the DC power is modulated with RF carrier and radiated from transmitting antenna onto "rectenna", which collects and converts the impinging power of microwave to available DC power. As shown in [9], five efficiencies are defined respectively to evaluate the efficiency of these five building blocks(Fig.1). The overall efficiency (end-to-end efficiency) is the ratio between available DC power at receiver and supplied DC power at transmitter, which is the product of these five efficiency values from each building block.

Antenna is a transducer to bridge circuit theory and field theory. Since the excitation weight of antenna array is normally controlled by circuit elements and transmission efficiencies are evaluated at circuit level, the powers are expressed in terms of voltage and current vectors. The definitions of power are firstly clarified in this section so that we can clearly set an optimization goal.

In antenna array system, each array elements is not independent and the radiated fields interfere to form the radiation pattern. In this way, in the far field, the array is

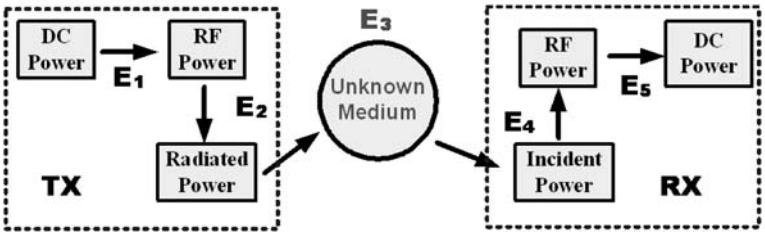

Fig. 1 Microwave power transmission system: E_1 to E_5 are power transfer efficiencies

treated as a single antenna and propagated in a spherical coordinate with the array at the origin. The total radiated power (P_{rad}) can be expressed in terms of the current fed at each port($\mathbf{I}$) and mutual impedance matrix ($\mathbf{Z}$). The real part of $\mathbf{Z}$ corresponds to the radiated energy while the imaginary part corresponds to the reactive energy stored in near field region.

$$P_{rad} = \frac{1}{2}\mathbf{V}^H\mathbf{I} = \frac{1}{2}\mathbf{V}^H\Re\{\mathbf{Z}_A^{-1}\}\mathbf{V} \tag{1}$$

The total power(P_Ω) can also be computed by taking the integral over the enclosing sphere with antenna at center. Moreover, the power focused at the angular region Ψ given by receive aperture (P_Ψ) is also defined for the beamforming optimization. These expressions can be similarly simplified into the product of vectors [14].

$$P_\Omega = \int_\Omega W_n dS \tag{2}$$

$$P_\Psi = \int_\Psi W_n dS \tag{3}$$

where W_n is Poynting flux density.

By energy conservation, the radiated power (P_{rad}) is equal to the power enclosed by the sphere (P_Ω), and is related to the input power by reflection coefficiency(Γ) of antenna ports: $P_{rad} = (1-|\Gamma|^2)P_{in}$. Normally the antenna impedance is matched to the port impedance so the reflection coeffieiency is approximately equal to 0 (in this condition, $P_{rad} = P_{in}$).

The incident power with matched load is summed up at the receiver side, as the incident field induces RF currents at each port of receive antenna. The transmission efficiency (E_3) in Fig. 1, which connects the transmit and receive array, is therefore optimized in power beamforming.

$$E_3 \triangleq \frac{P_{inc}}{P_{rad}} \tag{4}$$

In array synthesis theory, the beam collection efficiency (BCE) is usually used to evaluate the ability to shape the total power (P_Ω) towards the targeted angular region (P_Ψ) [14]. The overall efficiency is defined as the ratio between the total available RF power ($P_{L,tot}$) and the total input power at transmit array($P_{in,tot}$), which includes the efficiency of transmit antenna (E_2), transmission efficiency(E_3) and receive antenna (E_4).

$$BCE \triangleq \frac{P_\Psi}{P_\Omega} = \frac{P_\Psi}{P_{rad}} \tag{5}$$

$$\eta \triangleq E_2 E_3 E_4 = \frac{P_{out}}{P_{in}} \tag{6}$$

Since BCE is proportional to the transmission efficiency (E_3), BCE is usually the optimization goal instead of the transmission efficiency for the simplicity of mathematical formulation with array factor(AF). However, in the scenario with multipath and high-absorbing or reflection obstacles, the AF and BCE are not valid for optimization as the line-of-sight(LOS) is not available.

1.2 Transmission Efficiency based on Antenna Parameters

The electromagnetic field radiated from the antenna can be described as plane wave propagation in the far field, where the power of radiation decays as the square of distance. In most of wireless applications, the antenna operates in the region of far field and the transmission efficiency is computed in the way of link budget calculation with the help of the well-known Friis transmission equation. The complete version of Friis transmission equation is usually expressed as (7) in terms of antenna gain.

$$\frac{P_{rx}}{P_{tx}} = G_{tx} G_{rx} (\frac{\lambda}{4\pi R})^2 (1 - |\Gamma_{tx}|^2)(1 - |\Gamma_{rx}|^2) |\hat{a_{tx}} \cdot \hat{a_{rx}}^*|^2 \tag{7}$$

where G_t denotes the gain of transmit antenna and G_r denotes the gain of receive antenna. R is the distance between transmit antenna and receive antenna. $|\Gamma_t|$ and $|\Gamma_r|$ are the reflection coefficient of transmit and receive antenna respectively. $\hat{a_r}$ denotes the polarization vector of receive antenna while $\hat{a_t}$ denotes the incident wave electric field vector or polarzation vector of transmit vector in LOS propagation. The term $|\hat{a_t} \cdot \hat{a_r}^*|^2$ represents the polarization conversion loss in converting the incident wave into RF power available at antenna port. The antenna gain is proportional to the effective aperture size of antenna,

$$G = \frac{4\pi}{\lambda^2} A_{eff} = \frac{4\pi}{\lambda^2} \eta_{ap} A_{phy} \tag{8}$$

where A_{eff} is the effective aperture size and the A_{phy} is the effective physical size. η_{ap} is the aperture efficiency of the antenna. The aperture effieicny relates the physical aperture are to the effecive aperture area and can be treated as constant for a

given array element geometry.

$$\begin{aligned}\eta_{far} &= \frac{P_{rx}}{P_{tx}} = \frac{A_{eff,tx}A_{eff,rx}}{c^2}(\frac{f}{R})^2 \\ &= \eta_{ap,tx}\eta_{ap,rx}\frac{A_{phy,tx}A_{phy,rx}}{c^2}(\frac{f}{R})^2\end{aligned} \tag{9}$$

After rearranging the Friis transmission equation (Eq.(7), a more intuitive expressision can be expressed in terms of physical size and operation frequency in (9), assuming no polarization loss and negligible mismatch loss. This expression gives the design guideline of the phased array antenna. Given the range of propagation and the limitation of the array size, the higher frequency of operation leads to higher transmission efficiency. This conclusion contradicts our normal intuition in link budget calculation of wireless communication, that the lower frequency gives lower path loss. The reason for this contradictory conclusion is that, give the fixed physical size of array antenna, the number of antenna elements increased as with the decrease of wavelength instead of using single antenna as in wireless communication. Besides, for the use of consumer electronics, the receiver of wireless power is mobile and has to be as small as possible so the demand of smalller size receive array can be compensated by the larger size of transmit array from the observation of this equation.

However, the Friis equation is defined in the region of far field that is given by $R > \frac{2D^2}{\lambda}$, where D is the dimension of array aperture. It implies that, in most cases, the array antenna operates in the Fresnel near field region and incident wave is spherical wave instead of plane wave, if we attempt to achieve the higher transmission efficiency by increasing the frequency of operation and the larger size of transmit array. Another expression for estimating the transmission efficiency in the intermediate near field region is given in [20] and [1]. This expression is more accurate when the aperture size of transmit array is very large and more comparisions can be found in the book [20].

$$\eta_{near} = \frac{P_{rx}}{P_{tx}} = 1 - e^{-\tau^2} \tag{10}$$

where $\tau = \eta_{far}$ is equal to the Friis equation.

1.3 Transmission Efficiency based on Channel Transfer Function

This subsection presenets a general model in terms of the channel transfer equation and mutual impedance matrix. The microstrip patch antenna is taken as an example in our formulation and simulation, which is the most popular planar antenna because it is relatively inexpensive to manufacture and integrate with printed circuit design. In Fig. 3, the input voltage at the port of n_{th} patch antenna is denoted by $V_{in,n}$ and the voltage at the radiating slot of this patch is the transmitted wave $V_n = (1-\Gamma_n)V_{in,n}$,

where $\Gamma_n = (Z_A - Z_0)/(Z_A + Z_0)$.

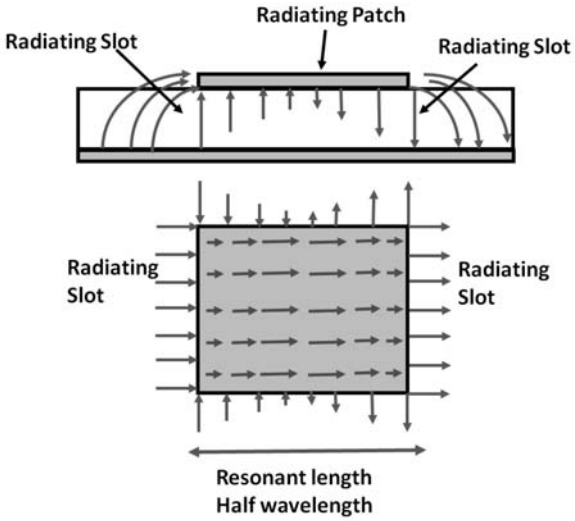

Fig. 2 Radiation of the patch antenna in TM_{10} mode: blue arrow is electric field and red arrow is current flow

From the model in [2] , the electric field, at any point $\mathbf{r}$, given by the n_{th} patch antenna of transmit array at $\mathbf{r}_n$, is expressed in terms of the locations, dimensions of patch and the voltage at radiating slots as Fig.. The microstrip antenna is a rectangular patch with width of W and length of L and the substrate thickness is h.

$$\mathbf{E}(\mathbf{r},\mathbf{r}_n) = \frac{-jV_n k_0 W e^{-jk_0 R}}{\pi R} F(\theta,\phi) \tag{11}$$

$$\mathbf{E}(\mathbf{r},\mathbf{r}_n) = \kappa V_n G(R)\mathbf{F}(\theta,\phi) \tag{12}$$

where $R = |\mathbf{r} - \mathbf{r}_n|$, $\kappa = (-jk_0 W)/\pi$ and $G = e^{-jk_0 R}/R$.
θ and ϕ are the spherical angles corresponding to the location $\mathbf{r}_n$. In the directivity pattern$\mathbf{F}(\theta,\phi)$, the origin of spherical angles for different patch elements should be the geometric center of the corresponding patch. However, since we have the far field approximation $\theta_1 \cong ... \cong \theta_M \cong \theta$ and $\phi_1 \cong ... \cong \phi_M \cong \phi$, the values of θ and ϕ corresponding to every transmit element can be approximated by the angle from the phase center of array to the observation point.

The directivity pattern $\mathbf{F}(\theta,\phi)$ has two orthogonal components $\mathbf{F}_\theta$ and $\mathbf{F}_\phi$.

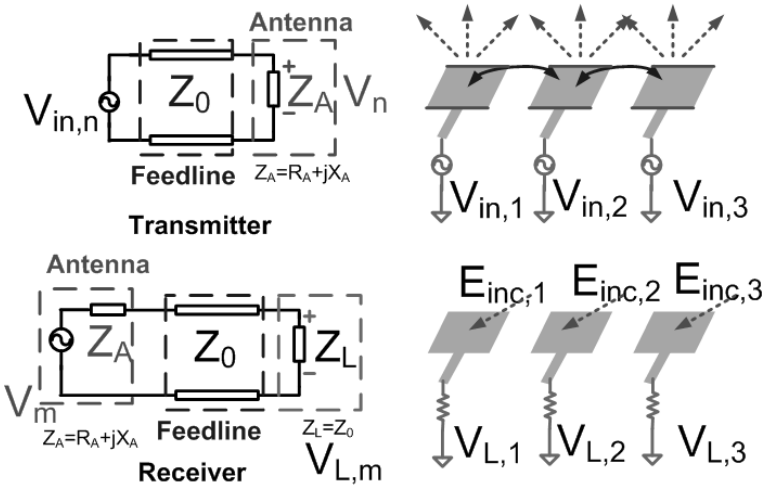

Fig. 3 Transmit and receive patch antenna array: $E_{inc,n}$ is the incident electric field onto the n_{th} receive antenna elements; $V_{in,n}$ is the input voltage at the port of n_{th} transmit antenna; Z_A is the impedance of transmit/receive antenna; $V_{L,n}$ is the available voltage at the load of receive antenna; Z_L is the load impedance of the receive antenna.

$$\begin{aligned}\mathbf{F}(\theta,\phi) &= \hat{\theta}F_\theta + \hat{\phi}F_\phi \\ \mathbf{F}(\theta,\phi) &= [\hat{\phi}cos\theta sin\phi - \hat{\theta}cos\phi]cos(khcos\theta) \\ &\quad \frac{sin(\frac{k_0W}{2}sin\theta sin\phi)}{\frac{k_0W}{2}sin\theta sin\phi}cos(\frac{k_0L}{2}sin\theta cos\phi)\end{aligned} \tag{13}$$

The electric field in Eq.(12) can be constructed coherently in space to cancel out the power flow in undesirable direction. Since the electric field is governed by the law of linear superposition, the incident electric field at the m_{th} receive patch antenna ($\mathbf{r}_m$) is denoted by the sum of electric fields due to input voltage at all M transmit elements.

$$\mathbf{E}_{inc}(\mathbf{r}_m) = \sum_{n=1}^{N} \kappa V_n G(|\mathbf{r}_m - \mathbf{r}_n|)\mathbf{F}(\theta,\phi) \tag{14}$$

By introducing the vector effective length $\mathbf{L}_{eff}(\theta_m,\phi_m)$ [16], the induced voltage at the m_{th} receive element is simply the dot product between incident field and effective length.

$$\begin{aligned}V_m &= \mathbf{E}_{inc}(\mathbf{r}_m)\cdot\mathbf{L}_{eff}(\theta_m,\phi_m) \\ &\approx \sum_{n=1}^{N} \kappa V_n G(|\mathbf{r}_m - \mathbf{r}_n|)[\mathbf{F}(\theta,\phi)\cdot\mathbf{L}_{eff}(\theta^{'},\phi^{'})]\end{aligned} \tag{15}$$

It is noted that, in the far field approximation, the angles θ_m and ϕ_m can be referred to the geometric center of receive array and the effective length of all the receive elements are approximately equal from the equal incident angles $\theta^{'}$ and $\phi^{'}$. In addition, since there is no widely-accepted theory to calculate the exact efficiency of power absorption at receive antennas [17], the effect of scattering or reradiation is not discussed in this paper and its effect is simply included into the polarization mismatch of incident field and the impedance mismatch at the load impedance. Hence, the transfer function from the input port to output load, which is actually the S parameters in numerical simulations, can be formulated as follows.

$$\begin{aligned} H_{mn} &= \frac{V_{out,m}}{V_{in,n}}|_{V_{in,j}=0 for j\neq n} \\ &= \kappa(1-\Gamma_n)G(|\mathbf{r}_m-\mathbf{r}_n|) \\ &\quad [\mathbf{F}(\theta_n,\phi_n)\cdot\mathbf{L}_{eff}(\theta_m,\phi_m)]\frac{Z_0}{Z_0+Z_A} \end{aligned} \tag{16}$$

At transmitter side, $(1-\Gamma_n)$ denotes the reflection at the input port of transmit antenna. At receiver side, $[\mathbf{F}(\theta_n,\phi_n)\cdot\mathbf{L}_{eff}(\theta_m,\phi_m)]$is the polarization factor while $Z_0/(Z_0+Z_A)$ is mismatch factor [16].
$G(|\mathbf{r}_m-\mathbf{r}_n|)$ is the Green's function, which represents the wave propagation from the transmit element to receive element. In free space, it can be simply taken as its simplest form $G=e^{-jk_0R}/R$ while, in complex medium, this function has to be modified to a different expression of Green's function accordingly[7].

The total RF power deliverable to the load can be added up over all the receive elements incoherently.

$$\begin{aligned} P_{out} &= \sum_{m=1}^{M}\frac{V_{out,m}V_{out,m}^*}{2Z_L} \\ &= \frac{1}{2Z_L}\sum_{m=1}^{M}\sum_{n=1}^{N}(V_{in,n}H_{mn})(V_{in,n}H_{mn})^* \\ &= \frac{1}{2Z_L}\mathbf{V}_{in}\mathbf{H}\mathbf{H}^H\mathbf{V}_{in}^H \end{aligned} \tag{17}$$

The total input power can also be computed at circuit level in terms of mutual impedance matrix in (1) and reflection coefficient $P_{in}=P_{rad}/(1-|\Gamma|^2)$. Hence, the overall RF transmission efficiency, which includes the efficiencies due to transmit antenna, receive antenna and wave propagation in medium, is computed as follows ($\eta=E_2E_3E_4$).

$$\begin{aligned}\eta &= \frac{P_{out}}{P_{in}} = \frac{(1-|\Gamma|^2)}{Z_L}\frac{\mathbf{V}_{in}\mathbf{H}\mathbf{H}^H\mathbf{V}_{in}^H}{\mathbf{V}_{in}\Re\{\mathbf{Z}^{-1}\}\mathbf{V}_{in}^H} \\ &\sim \frac{\mathbf{V}_{in}\mathbf{H}\mathbf{H}^H\mathbf{V}_{in}^H}{\mathbf{V}_{in}\Re\{\mathbf{Z}_A^{-1}\}\mathbf{V}_{in}^H}\end{aligned} \tag{18}$$

1.4 Experiment Study of Indoor MPT

Since the accuracy of the aforementioned models is to be validated, a wireless power transmission experiment is carried out in our lab environment with two array placed face-to-face with each other. To obtain the insight into the MPT in such a scenario, the complete MPT system is built with the detailed analysis of link budget.

Firstly, the indoor experiment is carried out with two standard gain horn antennas with the realized gain of 14 dB and the measured S_{21} (deembeded to the plane of antenna port) is tabulated as follows when the two antennas are facing with each other accurately. Moreover, it it noted that the dimension of the horn antenna is approximately $D = 0.2m$ so the far field condition is $R > \frac{2D^2}{\lambda} \approx 1.54m$ while the near field condition is $R > 0.62\sqrt{\frac{D^3}{\lambda}} \approx 0.24m$. This implies that the system operates in the Fresnel near field region, where the radiation pattern or spatial distribution of electromagnetic field varies significantly with the distance. From the Table 1, it is

Table 1 Measurement with horn antenna versus distance. The S_{21} reflects the power ratio at the network analyzer so the cable loss is extracted to deembed the reference to the antenna ports. The path loss is computed from Friis equation with unity antenna gain assuming the transmision with isotropic radiator.

Distance	0.6m	1.2m	1.8m	2.4m	3m
Deembeded S_{21}	-22dB	-27dB	-30dB	-31dB	-32dB
Path Loss	-50dB	-55dB	-58dB	-59dB	-60dB
Near Field Equation (10)	-30dB	-42dB	-49dB	-54dB	-58dB
Far Field Equation (9)	-15dB	-21dB	-25dB	-27dB	-29dB

found that the far field equation gives a closer estimation of transmission efficienc while the estimation error of near field equation is much larger. The reason for this is that the receiver is closer to the far field boundary than near field boundary. The general rule of determining which equation is stated in [20] as that the near field efficiency is more accurate when the value of τ is larger than 1.

Next, the prototype of MPT system including both transmitter and receiver is also built to study the contribution of real system losses. As shown in Fig.4, the full system includes the signal generator, power divider, transmit and receive antenna array, RF rectifier with load resistor and high power amplifier.

The transmit and receive antenna array are the same series-fed microstrip antenna array, which has 14 elements connected in series governed by the Chebyshev

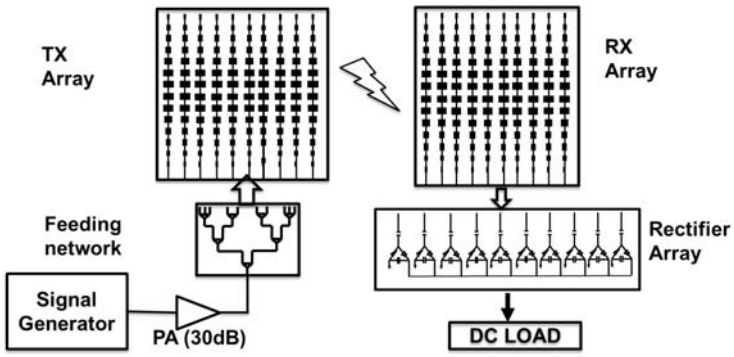

Fig. 4 Experimental configuration of the full MPT system

distribution of width tapering and operates in the resonant mode. In the other dimension, 10 input ports are connected in parallel with the spacing of half free space wavelength. At the transmitter side, the 10 parallel input ports are fed with a 10-way broadband power divider, which is made up of the cascaded 2 way Wilkinson power dividers and 3 way dividers. Therefore, the 10 ports of power divider are weighted rather than equally distrubted. This feeding network can reduce the sidelobe level (SLL) to some extent while achieving broadband power combining at the cost of increased insertion loss. The antenna array and the power divider are fabriated on two separate FR-4 printed circuit board (PCB). The antenna array gives the simulated realized gain of 25 dB, and the broadband power divider gives the measured -6.96 dB insertion loss of power division. Therefore, the total array with the power divider at the transmitter gives realized gain of approximately 19 dB. The power amplifier is a broadband high power amplifier by Mini-Circuits with typical power added efficiency (PAE) of 30% at 5.8 GHz and can output up to 1 Watt RF signal without distortion.

At the receiver side, the RF rectifier array is implemented with the single stage charge pump topology and converts the RF signal to DC power. The diode in the rectifier is the HSMS-286x surface mount schottky detector diode by Avago Technology, which gives the low series resistance of 6Ω. The single rectifier unit achieves up to 73% conversion efficiecny with this low loss diode. The rectifier array employs the hybrid of series and parallel power combining at DC, and is optimized to 20% to 40% conversion efficiency with the DC load of 150Ω and input signal of 0 dBm sinusoidal wave at 5.8GHz, which is the case in our measurement. It is noted that the efficiecny of rectifier varies with the input power level, input signal frequency, the way of DC power combining and DC load present to the rectifier, so the conversion efficiency keeps changing with the experimental condition.

The full system measurement is carried out with the separation distance of 3 meter between the transmitter and receiver. To find out the contribution of the system loss, each component of the whole system must measured one by one and, when the signal generator outputs the RF power of 0 dBm , the link budget can be estimated

as in Fig.5. To analyze the contribution of low efficiency, the total system losses are dissected in the view of a pie chart as shown in Fig.6.

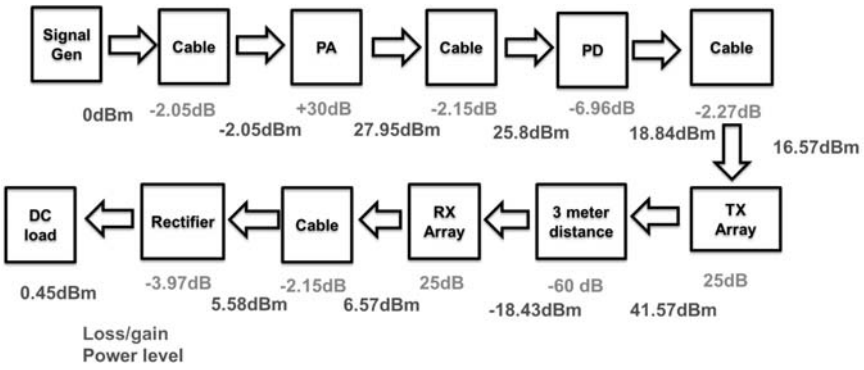

Fig. 5 The link budget of prototype system. The PAE of power amplifier is taken as 30% as given by the device specification while the conversion efficiency of rectifier array is taken as 40%. The distance between transmitter and receiver it taken as 3 meter. The path loss excluding antenna gain is estimated using the measurement in Table 1 and the radiation into wave proagation medium is labeld as radiation loss.

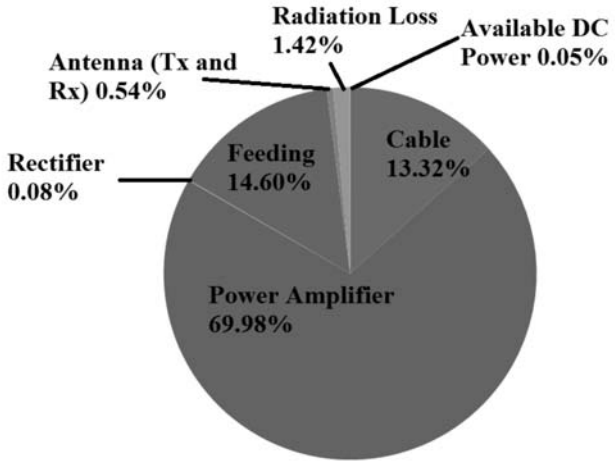

Fig. 6 Contribution of system losses:The measured output DC power is consistent with the estimated link budget in Fig.5.The total DC to DC transmission efficiency is computed as 0.068%.

From the analysis of system losses, it can be found that, because the total DC power at transmitter is almost equal to DC power consumption of power ampli-

fier, the upper limit of power loss is set by the PAE of power amplifier (PA) and the amount of this loss is fixed. Though the second and third largest power loss is contributed by the feeding network and RF cable as Fig.6, these losses can be effecitively reduced using the spatial power combining technique.

However, in spite of the high efficiency circuit design, the radiation loss will dominate the system loss and is hard to suppress. The degradation of efficiency is more serious when the LOS propagation is not available. When the LOS channel is blocked in the experiment, the loss of the fixed beam array increases by more than 20 dB according to our experiment. The only possible solution to high transmission efficiency is adaptive beamforming array. Techniques for adaptive array will be discussed in the following Section 2.

2 Reivew of Optimal Beamforming Techniques

The antenna beamforming is achieved through the coherent operation of antenna elements so the excitation weight of each element determines the performance of beamforming.

2.1 Array Factor Optimization

In traditional beamforming based on AF synthesis, the antenna elements are assumed to be have the same radiation pattern and accurately postioned. The steering vector $\mathbf{v}_s = [e^{ik(ux_n+vy_n)}]$ is used to yield the AF $F(u,v) = \sum_{n=1}^{N} w_n e^{ik(ux_n+vy_n)}$,where (u,v) identifying the angular region . Since the power of AF is proportional to the spatial distribution of the radiated power, BCE is expressed in terms of power of AF and a closed form expression of BCE is derived for the planar array case by Oliveri et.al [14] .

$$BCE = \frac{\int\limits_{\Psi} \sum_{n=1}^{N} w_n e^{ik(ux_n+vy_n)}}{\int\limits_{\Omega} \sum_{n=1}^{N} w_n e^{ik(ux_n+vy_n)}} = \frac{\mathbf{w}^H \mathbf{A} \mathbf{w}}{\mathbf{w}^H \mathbf{B} \mathbf{w}} \tag{19}$$

where $B_{mn} = 4\pi sinc(k\sqrt{(x_m - x_n)^2 + (y_m - y_n)^2})$ and $A_{mn} = 4\pi u_0 v_0$ $sinc(k(x_m - x_n))sinc(k(y_m - y_n))$

This approximation greatly reduces the computation time at the cost of accuracy. However, for other structures and spacings of array, the closed form expression is not available and the numerical integral of powers has to be performed, which may take a long time to approach an optimal solution. In reality, the radiation pattern of array element is never the same due to mutual coupling, edge effect and manufacturing process. More importantly, this technique is not valid for power optimization if the array is not regular shape with known position [14].

2.2 Retrodirective Array/Phase Conjugate Array

Retrodirective Array is the array to reflect the incident plane wave toward the source direction without any prior information on the source location. The retrodirective array works in the following way: the receive array/interrogate antenna out a probing signal and then transmit array retransmits the amplified signal towards receiver by taking phase conjugate of the observed probing signal. Since the phase conjugating functionality can be implemented at RF frequency with hardware, its popularity arises from the automatic beam steering without any computational algorithm (i.e. digital signal processing hardware). Although this technique is also adaptive to the propagation channel, it only works for a fixed frequency. The array calibration becomes problematic, depending on the hardware design.

2.3 Adaptive Array Digital Beamforming

Digital beamforming is more powerful and flexibile than conventional phased array at the expense of hardware complexity and cost. However, if the estimation of channel characteristics is enabled by the additional receive antennas, the adapative signal processing results in a more powerful beamforming transmitter and flexibile beamforming formulation regardless of array shape and position. Digital beamforming based on the channel estimation is also an important technique to enhance the signal-to-interference ratio (SIR), signal-to-noise ratio (SNR) and the intersymbol interference (ISI) in the in MISO or MIMO communciation.

The time reversal(TR) technique has been studied extensively in wireless communication by many researchers [11], as this scheme can improve SNR greatly in multipath and rich scattering environment. The receivers send a probing signal to transmitter for channel estimation and the transmitters convolve the time reversed channel impulse response $h(-t)$ with the transmitted signal $s(t)$. The received signal will be equal to the convolution between the transmitted signal $s(t)$ and the autocorrelation of the channel impulse response. Eq.(20) indicates that the energy will be spatially focused at the target receiver in any environment. When the receiver has multiple antennas, this TR beamforming technique is not valid for energy focusing.

$$y(t) = s(t) * h(-t) * h(t) = s(t) * R(t) \tag{20}$$

The eigen-beamforming is an optimal scheme for maximizing the average SNR [24] in the narrowband MIMO. Nevertheless, the optimizaton of SNR happens at the output of matched filter instead of the summed power at the receiver. Besides, it is noted that the maximization is implemented with the coding scheme, which results in the spectrum spread. For this reason, this technique is not applicable for adaptive beamforming in MPT, which requires the continuous wave transmission.

$$SNR = \frac{E\{\mathbf{h}^H \mathbf{C}^H \mathbf{C}\mathbf{h}s\}}{E\{\mathbf{h}^H \mathbf{C}^H \mathbf{n}\mathbf{n}^H \mathbf{C}\mathbf{h}\}} \tag{21}$$

where $\mathbf{h}$ is the matrix of channel impulse response in time domain and $\mathbf{C}$ is the coding scheme of eigen-beamforming. $\mathbf{n}$ is the Gaussian noise and s is the baseband signal carrying information.

Furthermore, the time revesal scheme is analyzed using the model of Green's function in the frequency domain [6] [8] ,as the time reversed signal is equivalent to the complex conjugate in frequency domain. The paper [6] and [8] demonstrate that the communication efficiency can be improved with the proposed beamforming scheme in theory and in experiment, respectively. To our knowledge, the specific application of adaptive beamforming for WPT has not been reported yet.

3 Time Reversal Eigenmode Beamforming

The classic array synthesis technique is developed based on the model of AF with the assumption of equal element pattern. As is widely known by antenna designer, the mutual coupling leads to the the unequal pattern especially for the edge element. For the array with unequal element and arbitrary location, the AF is no longer valid and the adaptive array processing has to be employed for the array synthesis using the knowledge of probing channel characteristics. However, the previous studies of adaptive beamforming are developed for improving the signal-to-noise (SNR) ratio or channel capacity based on MIMO wireless communication and no discussions on how to devise an adaptive algorithm for MPT. This section presents a modified algorithm for MPT based on the time reveral signal processing techniques. Beside, it will also be proved as a new optimal array synthesis method without the prior knowledge of element spacing and positions.

3.1 Pseudo Transmission Efficiency

To implement the adaptive optimization of transmission efficiency, we propose the pseudo transmission efficiency(PTE) as an alternative optimization goal. PTE is the ratio between the total RF power available at the receive array and incoherent sum of the input power over all transmit elements.

The incoherent sum of radiated power takes the sum of input power at each radiator independently and is only physical for special case that the mutual impedance matrix is diagonal matrix ($P_{sum,in} \neq P_{in}$). However, the incoherent power is used in communication society for evaluation of power in wireless communication by neglecting the mutual coupling effect. Similarly, the incoherent sum of radiated power is related to input power ($P_{sum,rad} = (1 - |\Gamma|^2)P_{sum,in}$).

$$P_{sum,rad} = \frac{\mathbf{V}^H \mathbf{V}}{2R_{rad}} = \frac{1}{2}\mathbf{V}^H \Re\{diag[\mathbf{Z}_A^{-1}]\}\mathbf{V} \tag{22}$$

$$PTE \triangleq \frac{P_{out}}{P_{sum,in}} \tag{23}$$

PTE is not a physical efficiency, but the difference between PTE and η (Eq.(18) is negligible if the real part of mutual coupling impedance terms are sufficiently small. When the adjacent antenna elements are weakly coupled to each other, the transmit channels are uncorrelated with each other. The correlation between transmit channels are expected to be low in both MPT and MIMO communication. While the envelope correlation coefficient(ECC) is an indicator of the MIMO antenna design, the independency of MPT array is reflected by the ratio between the radiated power and the coupled power dissipation in the following Eq.(24). It is noted that this correlation power factor is related to the complex excitations of the array elements and the power ratio R increases as with the improved isolation between adjacent elements.

$$R(\mathbf{V}_{in}) \triangleq \frac{\sum_{i=1}^{N} v_i \Re\{y_{ii}\} v_i^*}{\sum_{j=1}^{N}\sum_{i=1,i\neq j}^{N} v_i \Re\{y_{ij}\} v_j^*} \tag{24}$$

To verify this assumption quantitatively, a simple 2 x 2 rectangular array is simulated in Ansys HFSS and the expored Y parameter is used to compute the correlation power factor with several complex excitation combinations. These five excitation vectors have the uniform magnitude but random linear phase progression. Fig.7 shows that the exact value of correlation power factor is dependent on the excitation vector but the average increases with the array element spacing, which is equivalent to the isolation between two elements. The improvement of mutual coupling can also be implemented by the techniques of enhancing ECC in MIMO antenna design.

In Fig.8, the error between incoherent power sum ($P_{sum,in}$) and physical input power(P_{in}) is defined as $Error \triangleq |(P_{sum,in} - P_{in})/P_{sum,in}|$ and the error is plotted for different excitations as in Fig.7. The average of the five excitations shows that the average error is well below 5% when the array spacing is greater than the half free space wavelength. In summary, the plots in Fig.7 and Fig.8 quantitatively justify why the PTE gives a good estimation of transmission efficiency for weakly coupled array.

3.2 Transmission Efficiency Optimization

Since the correlated power is sufficiently low in most array setup, this paper will discuss the optimization of PTE instead of either η or BCE. If the PTE is rearranged, Eq.(23) can be simplified as in (25).

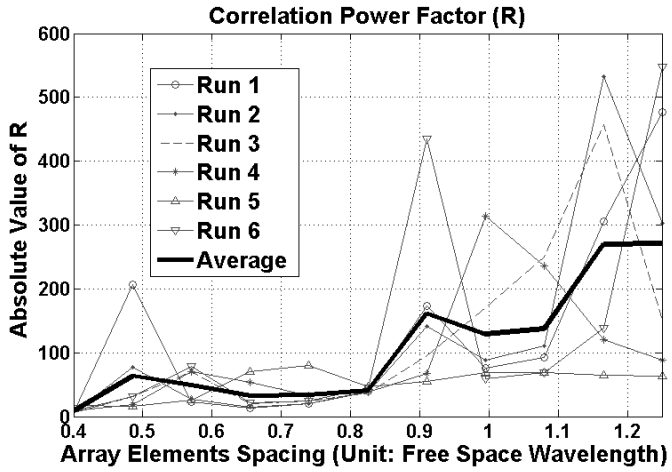

Fig. 7 Correlation power factor (R): the average correlation power factor increases as with the increase of element spacing.

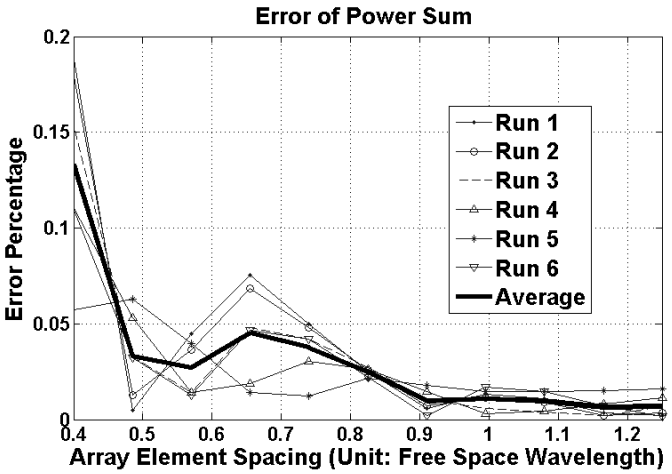

Fig. 8 Error percentage of incoherent sum: the average error decreases as with the increase of element spacing

$$
\begin{aligned}
PTE = \frac{P_{out}}{P_{sum,in}} &= \frac{(1-|\Gamma|^2)}{Z_L}\frac{\mathbf{V}_{in}\mathbf{H}\mathbf{H}^H\mathbf{V}_{in}^H}{\Re\{Z_{rad}^{-1}\}\mathbf{V}_{in}\mathbf{V}_{in}^H} \\
&\sim \frac{\mathbf{V}_{in}\mathbf{H}\mathbf{H}^H\mathbf{V}_{in}^H}{\mathbf{V}_{in}\Re\{diag(\mathbf{Z}_A)^{-1}\}\mathbf{V}_{in}^H} \\
&\sim \frac{\mathbf{V}_{in}\mathbf{H}\mathbf{H}^H\mathbf{V}_{in}^H}{\mathbf{V}_{in}\mathbf{V}_{in}^H}
\end{aligned}
\tag{25}
$$

From Eq.(18) and Eq.(25), it is clear that the ultimate goal of achieving optimal transmission efficiency is to solve the eigenvalue problem $\mathbf{R}_Z\mathbf{P}\mathbf{V_{in}} = \lambda\mathbf{V_{in}}$, where $\mathbf{P} = \mathbf{H}^H\mathbf{H}$ and $\mathbf{R}_Z = \Re\{\mathbf{Z}\}$. $\mathbf{V_{in}}$ is the input voltage, which also corresponds to the eigenvector of this problem. This is a Rayleigh Quotient and the eigenvalues of $\mathbf{R}_Z\mathbf{P}$ give the possible range of the transmission efficiency η. From Min-Max Theorem, it is known that the dominant eigenvector (the eigenvector corresponding to the largest eigenvalue) maximizes the transmission efficiency η.

$$\mathbf{V}_{in,opt} = arg[\max_{\mathbf{V}_{in}} \frac{\mathbf{V}_{in}\mathbf{H}\mathbf{H}^H\mathbf{V}_{in}^H}{\mathbf{V}_{in}\Re\{\mathbf{Z}^{-1}\}\mathbf{V}_{in}^H}] \tag{26}$$

However, the mutual impedance matrix can only be estimated from measurements but the measurement is difficult if the number of array elements are very large so finding the matrices in this eigenvalue problem is a difficult task.

$$\mathbf{V}_{in,opt} = arg[\max_{\mathbf{V}_{in}} \frac{\mathbf{V}_{in}\mathbf{H}\mathbf{H}^H\mathbf{V}_{in}^H}{\mathbf{V}_{in}\mathbf{V}_{in}^H}] \tag{27}$$

Therefore, as discussed above, we may think of optimizing the PTE as an alternative goal because it can be computed from the signal levels observed at the input ports. This method is validated in Fig.8 as the error between η and PTE is expected to be negigibly small for the array with large spacing. In this way, another eigenvalue problem is formulated $\mathbf{P}\mathbf{V}_{in} = \lambda\mathbf{V}_{in}$. The Min-Max Theorem is also applicable for this as Eq.(27). In most cases, the maximization of PTE yields the maximal values of transmission efficiencies. Hence, the next challenge is how to devise an algorithm to approach this optimal eigenvector excitation.

3.3 Time Reversal Eigenmode Beamforming

Time reversal signal processing technique is derived from the research on acoustic focusing effect with time reversal mirror(TRM) by M.Fink [3, 4]. This principle focuses the energy thanks to the reciprocity of wave equation: the TR (using a negative time) of the wave functions's solution is also a solution to this equation as long as the media is slowly varying, reciprocal and linear. When the TRM emits the plane wave towards a passive scatterer and observes the the scattered signal, the emitted energy by TRM can be focused to this scatterer by retransmit a time reversed copy of observed signal. If the process is iterated, the energy become more and more focused on this passive target. This technique has been developed into applications including wireless communication and radar imaging in cluttered and complex medium with computational iterative process [22, 7, 18, 8].

If the channel transfer function between transmit and receive antenna can be measured in real time, the iterated time reveral process can be performed with a

simple eigendecomposition process as discussed in [7]. Thus, the proposed method requires the probing of channel transfer matrix and digital beamforming architecture. Basically, the RF hardware of MPT system is similar to the massive MIMO communication as in Fig.9 [21]. In such a power transmission system, the communication module is integrated with the power delivery module and used to probe the channel characteritics as MIMO communciation. Given a transmit array of N elements and a receive array of M elements, the process of the proposed technique is stated as follows.

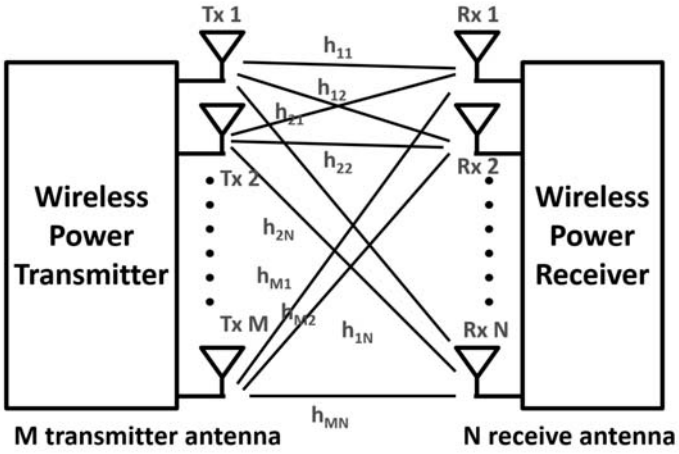

Fig. 9 Time reversal eigenmode beamforming system

- **Measurement of transfer matrix H(M-by-N)**
  The probing signal is an impulse waveform $s_n(t)$ spanning over the power transmission band and sent from each receive array elements one by one. The observed signal is recorded simultaneously at all the transmit elements and the recorded transient signal $y_m(t)$ is tranformed to frequency domain $Y_m(\omega)$ through Fourier Transform. Then the recorded signal is normalized to the probing signal as $h_{mn}(\omega) = Y_m(\omega)/S_n(\omega)$. $h_{mn}(\omega)$ is defined as the channel transfer function in frequency domain between the n_{th} element of transmit array and m_{th} element of receive array.
- **Construction of transfer power matrix P (N-by-N)**
  The transfer functions h_{mn} at the frequency of ω are rearranged into the matrix format as $\mathbf{H}(\omega)$.

$$\mathbf{H}(\omega) = \begin{bmatrix} h_{11} & h_{12} & h_{13} & \dots & h_{1N} \\ h_{21} & h_{22} & h_{23} & \dots & h_{2N} \\ \vdots & \vdots & \vdots & \ddots & \vdots \\ h_{M1} & h_{M2} & h_{M3} & \dots & h_{MN} \end{bmatrix} \tag{28}$$

The transfer matrix is used for the computation of the transfer power matrix($\mathbf{P}(\omega)$).

$$\mathbf{P}(\omega) = \mathbf{H}(\omega)^H \mathbf{H}(\omega) \tag{29}$$

- **Calculation of dominant eigenvectors(corresponding to largest eigenvalue)**
  The eigenvector of the transfer power matrix can be found through the numerical eigenvalue decomposition of measured data. As discussed before, the eigenvector that corresponding to the largest eigenvalue leads to the maximization of PTE and will be used for beamforming.

$$\mathbf{P}\mathbf{V}_{in,1} = \lambda_1 \mathbf{V}_{in,1} \tag{30}$$

- **Power delivery according to dominant eigenvector**
  Each element in the eigenvector $\mathbf{V}_1$ corresponds to the complex excitation of one antenna element. Since, in most cases, the single tone signal is used for wireless power transmission, the sinusoidal wave at the frequency of ω is weighted with the dominant eigenvector as follows.

$$y_m(t) = \mathfrak{F}^{-1}\{v_{1m}(\omega)\} = |v_{1m}(\omega)| sin(\omega t + \angle v_{1m}(\omega)) \tag{31}$$

The proposed scheme is implemented with the digital beamforming architecture so the synchronized transmitters synthesize the desired transmit signal $y_m(t)$ with analog-to-digital convertor(ADC) and feed into each transmit elements for power beamforming. It is noted that, in the real scenario of MPT, the available frequency of power transmission spans over a bandwidth of hundreds of megahertz while only a single carrier frequency is needed. In order to maximize the transmission efficiency, the eigenvalues of transfer power matrix over the available bandwidth can be compared to find at which frequency the power transmission has lowest propagation loss for the given environment.

The TR eigenmode technique have a drawback that is the susceptibility to interfering source. When there are multiple receivers requesting power transmission, the transmitter has to characterize the propagation channel corresponding to these receivers one by one and determine which frequencies are allocated to these receivers based on the frequency dependent eigenvalues corresponding to the receivers. After haveing determined the complex excitations, the simultaneous power transmission can be implemented by superimposing two signals at the baseband. For example, the m_{th} transmitter directly synthesize the signal which simultaneous power transmission to two receives as $y_m(t) = |v^1_{1m}(\omega_1)| sin(\omega_1 t + \angle v^1_{1m}(\omega_1) + |v^2_{1m}(\omega_2)| sin(\omega_2 t + \angle v^2_{1m}(\omega_2))$. In this way, the transmitter generates dual beams at two different frequencies pointing towards two receivers.

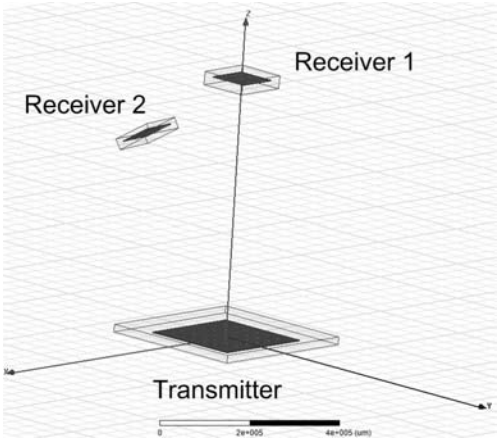

Fig. 10 Simulation in HFSS-IE. The rectangular patch array antennas are used for both receiver and transmitter. The positions of transmit elements are randomized.

4 Numerical Examples

The paper [14] reports that the BCE can be up to 99% by evaluating the power of AF. However, as discussed in Section 2 the efficiency derived from AF is not valid when the element pattern is not equal. To compare the effectiveness of different beamforming technique, the numerical simulation in different experiment setup is carried out in Ansys HFSS. The experimental verification of transmission efficiency and channel transfer function is extremely challgening and costly for large scale array beamforming. In this paper, the electromagnetic simulation is carried out in HFSS-IE, which is a new module based on Method of Moment-Integral Equation (MoM-IE) and designed for electrically large simulations.

As shown in Fig. 10, microstrip rectangular patch antenna is chosen for investigation as a representative of directive antenna rather than isotropic radiator. In HFSS, each antenna is placed on the planar Duroid 5870 substrate so each element has an image due to ground plane. Its radiation pattern of each antenna is modelled in the previous formulation. The field distribution on the virtual spherical air box is shown in Fig.13 to illustrate the power distribution in space. The amplitude and phase of exicitation is modified in the postprocessing function of HFSS according to the calculation of our proposed formulation.

Due to the intensive computation cost and limitation of computer memory, the 6 by 6 microstrip array is examined to make comparison with our theoretical model and the power transfer frequency is taken at 5.8 GHz in HFSS simulation. In the postprocessing, the excitations at each port can be specified with both amplitude and phase and the resultant beam pattern is obserbed in far field. The followings are several examples to show the advantages of the propsed schme with the aid of comparison table and figures.

4.1 Arbitrary Array Beamforming in Free Space

In the first example, the beamforming techniques are evaluated in free space in terms of several transmission efficiencies (η, η_{near}, η_{far} and PTE) and spatial distribution of electric field. Four beamforming techniques are chosen for investigation: uniform excitation, phase conjugate(same as retrodirective array), the proposed method, and AF synthesis technique described in [14].

In the HFSS simulation setup, the transmit arrray is arbitrarily positioned 6-by-6 antenna array as in Fig. 11, the inset of which shows the resultant arbitrary array for beamforming. The random spacing is generated by the nornmal distribution function of Matlab with the mean of $0.65\lambda_0$. The receive array is 3-by-3 rectangular array with the spacing of $0.65\lambda_0$ in both x and y direction. The receiver is located at a distance 0.5m from the center of transmit array and takes the angular area of 0.1×0.1 receive aperture, which is defined as $-\arcsin(0.1/2) \leq \theta \leq \arcsin(0.1/2)$ and $-\arcsin(0.1/2) \leq \phi \leq \arcsin(0.1/2)$)in spherical coordinate. It is noted that, in this case, the receive array is located in the Fresnel near field region because the distance between receiver and transmitter is between the far field ($\frac{2D^2}{\lambda} \approx 2.18m$) and near field boundary ($0.62\sqrt{\frac{D^3}{\lambda}} \approx 0.31m$). As the exact position of arbitrary array is not available, the mean spacing is taken for the formulation of AF. Therefore, the degradation of beamforming is expected due to the random phase error.

To compute the beamforming efficiency, the power density can be integrated

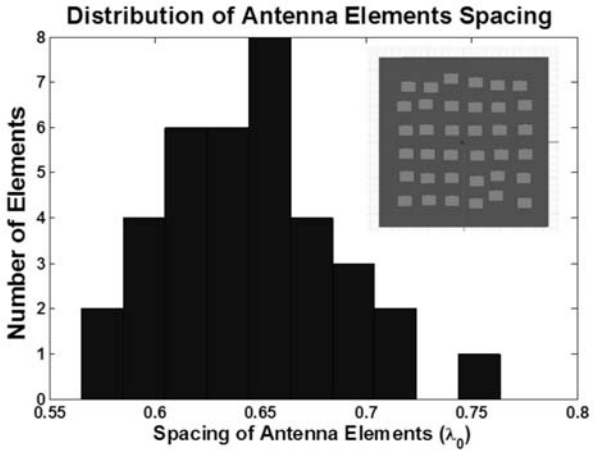

Fig. 11 Spacing distribution of randomly positioned antenna array: the mean of element spacings is $0.65\lambda_0$

over angular regions(Ψ) to obtain the power focused into the target area. It is noted that, when we compute the spatial power flow, the transmit antenna is simulated without receive antenna with finite element method(FEM) only and enclosed with

a upper hemisphere of radius 0.5m. Then the BCE (Eq.(5)) is computed to evaluate ability of shaping power beam into angular regions of 0.1×0.1 receive aperture. Besides, the received power and transmitted power are computed from mutual impedance matrix and S parameters are used to evaluate the transmission efficiency (Eq.(6)). For comparison, the inchorent sum of transmitted power is obtained from simulation and used for the computation of PTE as Eq.(6).

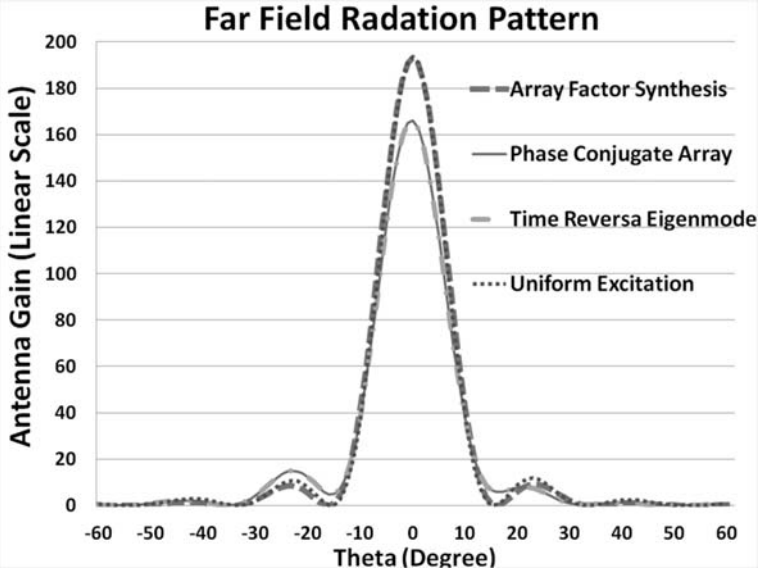

Fig. 12 Far field radiation pattern of transmit array with different beamforming techniques:max array gain in linear scale can be read from radiation pattern as 165.82, 177.16, 193.35 and 193.41 for the techniques of phase conjugate array, TR eigenmode, uniform excitation, and AF synthesis, respectively.

FEM simulation solves the far field antenna pattern with different complex excitations as in Fig.12. The max antenna gains can be read from radiation pattern as 165.82, 177.16, 193.35 and 193.41 (in linear scale) for the techniques of phase conjugate array, TR eigenmode, uniform excitation, and AF synthesis, respectively. These four beamforming techniques gives the effective aperture for the calculation in Eq.(9) and Eq.(10). The AF synthesis technique and uniform excitation give much higher gain and narrower beamwidth. From the models based on antenna parameters, it implies that these two techniques give higher transmission efficiency with the specific equations. However, the HFSS-IE simulation shows a controdictory results. The AF synthesis and uniform excitation result in the significant leakage of the real power flow (Fig.13 if the spatial electric field distribution is plotted on the enclosing hemisphere. The phase conjugate and TR eigenmode techniques have lower far field gain but focuses most of power into the region of receive aperture. For this reason, Table 2 shows that the model based estimation (either η_{near} or η_{far}) overestimates

the efficiency if it is compared with the simulated efficiency. The discrepancy is attributed to the wide main beam at the cost of lower gain so that the adapative beamforming directs more integrated power into the targeted area.

Futhermore, Table 2 shows that either phase conjugate array or time reveral

Table 2 Comparison of different optimization techniques for MPT in free space

Beamforming Method	BCE ($0.1 \times$ 0.1)	PTE	η	η_{near}	η_{far}	Gain (linear)
Uniform	21.37%	34.18%	18.50%	50.64%	70.59%	193.41
Phase Conjugate	33.05%	45.82%	25.14%	45.47%	60.65%	177.16
TR Eigenmode	33.22%	45.86%	25.22%	45.41%	70.59%	165.82
AF Synthesis	22.64%	36.58%	18.91%	50.63%	60.52%	193.35

eigenmode technique leads to higher transmission efficiency η especially in the case that the position of antenna elements is not available. It also verifies that the assumption of negligible correlated power dissipation is valid in adaptive beamforming and shows their advantages over the classic array synthesis.

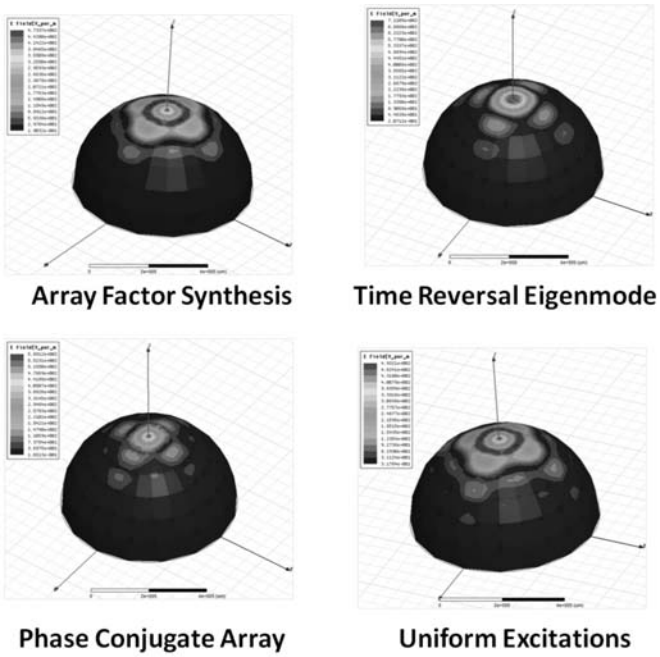

Fig. 13 Spatial power distribution from different beamforming methods: significant amount of power leakage appears for the AF synthesis and uniform excitations. The enclosing sphere shows the spatial distribution of the real power flow in the region of Frensnel near field region.

4.2 Arbitrary Array Beam Steering

The previous section demonstrates the potential of maximizing transmission efficiency when the receive array at the scan angle of 0 degree. At this scan angle, the transmit array gives the largest gain and the consequent transmission efficiency over any other beam pointing angles. In our analytical model, although the propagation channel is irrelevant with the location of scan angle, the synthesized beam by adaptive technique has the beam pointing error in some cases as discussed by [23]. Therefore, it is worthy of studying the impact of steering the beam away from the center.

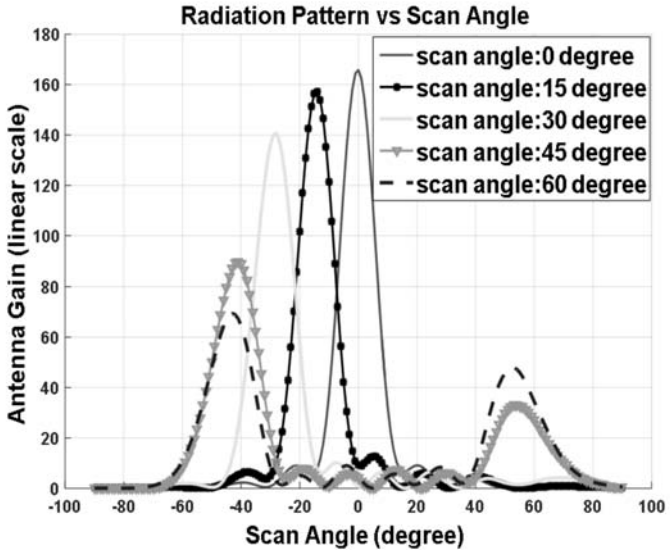

Fig. 14 Antenna pattern over different scan angles: grating lobe becomes large for the scan angle of $\theta = 45^o$ and 60^o; for the scan anlge of 60^o, the main beam cannot be steered to the direction of receive aperture.

In this subsection, the positions of transmit array elements are the same as last section while the receive array is rotated along the x axis to create different receiving angles. Fig.14 shows the beam steering towards the receive array based on the time reveral eigenmode technique. The main beam is steered to the angular region without the grating lobe where the receiver is until the scan angle is greater than 30^o. The limited scan angle is due to array spacing of $0.65\lambda_0$. According to the array theory, the maximum scan angle can be computed from the array spacing as $\theta_{max} = arcsin(d/\lambda_0 - 1) = arsin(0.538) = 32.57^o$. It is noted that, for the scan angle of 45^o, the most of power flows towards to the direction of receive array with the significant grating lobe at the symmetric location. However, when the scan angle moves further to 60^o, the main beam cannot be steered to the direction of receiver

any more. In fact, this phenonmenon is attributed to the scan blindness due to surface wave and can be mitigated by the proper antenna elements design with cavity backing and so on. The beam scanning pattern given by the adaptive array technique also presents the degradation of array gain, which is called the scan loss. The simulated gains at the angle of 0^o, 15^o, and 30^o, are 165.8, 157.3 and 140.6, respectively. The gain degradation is close to the scan loss equation $cos(\theta)$ (θ is scan angle).

From the aforementioned analysis, it can be found that the beam scanning leads to the drop of array gain, which is also predicated by the model of AF. As a consequence, Fig.15 shows that the transmission efficiency also drops as with the increase of scan angl. Given a fixed channel transfer matrix, the TR eigenmode technique gives a maximization of PTE and the consequent transmission efficiency η. However, the maximum value of η is limited by the array setup and propagation medium, no matter what complex excitation vector is. The limitation of array beam scanning is discussed using the model of Plane wave impulse response Element Patern in [23].

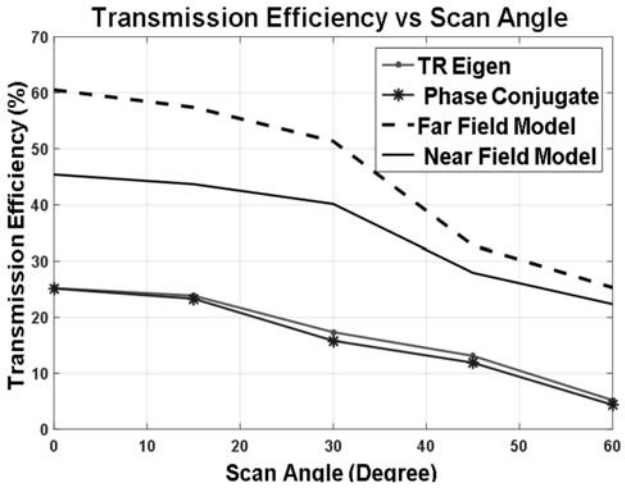

Fig. 15 Transmission efficiency over different scan angles. The near field and far field models overestimate the transmission efficiency while the PTE has much better accuracy.

4.3 Arbitrary Array Beamforming in Multipath Environment

In this subsection, an obscured propagation channel is studied to demonstrate the advantages of TR eigenmode technique in multipatch environment. In this numerical example, a PEC(perfect electric conducting) spherical obstacle is inserted (Fig. 16) with a diameter equal to the diagonal length of receiveaperture. This example has

also been formulated and discussed for the application of wireless communication in [8] and [6].

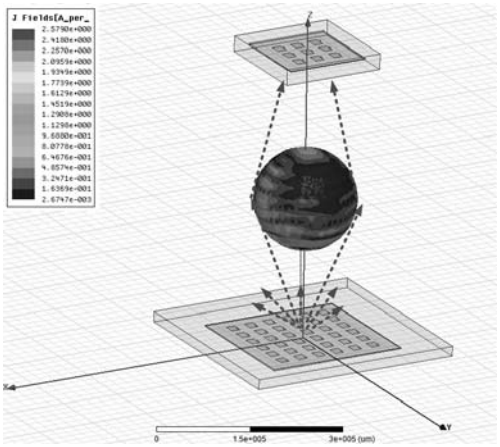

Fig. 16 Wireless power transfer behind PEC spherical obstacle. No LOS propagation path is available

Table 3 Comparison of different optimization techniques for MPT behind PEC spherical obstacle

Beamforming Method	Uniform	Phase Conjugate	TR eigenmode	AF Synthesis
η	2.23%	5.22%	5.85%	2.44%
PTE	3.12%	5.96%	6.39%	3.33%

The PTE and transmission efficiency are tabulated as Table 3 for four different techniques. In this case, if the array synthesis and uniform excitation techniques are not well-defined and shown for the purpose of comparison . Because the receiver is located in the region shadowed by the obstacle and no direct beam can be formed towards the receiver, the shaping of main beam towards any direction leads to a large amount of backward scattering. Nevertheless, the advantage of phase conjugate and TR eigenmode stands out in the comparison table. These two techniques gives several times greater efficienies (both η and BCE) over the other two techniques. Given the same norm of input power, the eigenmode method has approximately 10% higher efficiencies over the phase conjugate method (Table.3). It can be expected the improvements of efficiency from TR-Eigenmode method will be even more significant as with the increase of propagation channel due to multipath environment.

In Fig.16(a) and (b), the far field pattern from TR eigenmode and phase conjugate technique is computed with the results from FEM in HFSS. The reason why

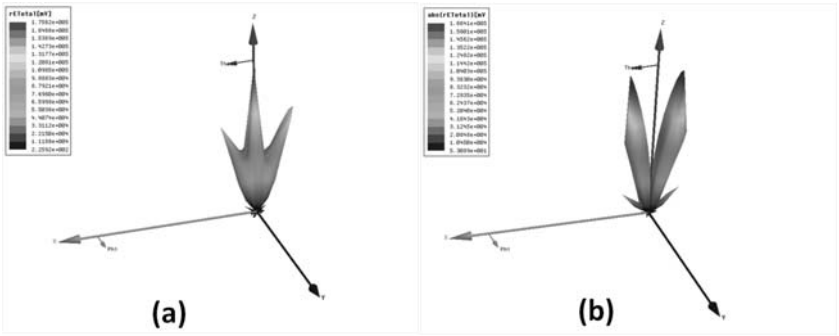

Fig. 17 Array beamforming with the presence of spherical obstacle:(a)radiation pattern from phase conjugate (b) radiation pattern from time reveral eigennmode. A significant main lobe exists in (a) and results in the propagation loss.

TR eigenmode technique is better than phase conjugate technique is shown apparently in Fig.16. Instead of one main beam in traditional beamforming technique, two beams are generated by the eigenvector excitations.The dual-beam maximizes the diffracted wave towards receiver while it minimizes the reflection by the obstacle. The phase conjugate technique, on the other hand, still maintains a main beam in the direction of LOS, apart from two side beams. Therefore, a portion of power is reflected back due to the existence of main beam. In Fig. 16, the induced surface current in MoM-IE method gives an implication of how the two side beam makes use of diffractions.

In short, the TR eigenmode method is the best adaptive array synthesis technique for MPT in the channel with multipath.

5 Conclusion

In this chapter, the wireless power transmission system is formulated in terms of the circuit theory and the field theory. The clarification of definitions on powers and efficiencies implies the challenges of estimating the transmission efficiecny. For this reason, the classic model of transmission efficiency based on antenna parameter is reviewed while another transmission equation is presented in terms of the channel transfer function and mutual impedance matrix. Then the experimental study of transmission efficiency is carried out in an indoor environment, which is a rich scattering and multipath environment. The quantitative study of transmission efficiency in experiment shows that the adaptive array beamforming is demanded to improve the MPT in a complex environment.

Furthermore, the exact transmission efficiency is approximated with pseudo transmision equestion(PTE) as the coupled power dissipation is sufficiently small if the array spacing is greater than half wavelength. Based on this approximation,

an optimal method is derived from time reveral signal processing technique. As the iterative TR process achieves spatial focusing effect through the automatic probing the channel characteristics, this property enlightens us with its application in the wireless power transimission. Then the iterative process is implemented computationally with eigendecomposition process since the channel transfer matrix can be measured and processed. Based on this principle, the time reveral eigenmode technique is proposed and validated with numerical examples. The MoM-Integral Equation was employed to demonstrate the advantages of the proposed techniques due to the prohibitive cost of large phased array. From the simulation results, it has been shown that the proposed scheme gives an optimal transmsision efficiency for an array with unequal element pattern and arbitrary position. Moreoever, the simulation also shows that this method is applicable for the receivers located in either far field or near field region while conventional array synthesis assumes the far field propagation. Most importantly, we have shown that the TR eigenmode technique can improve the transmission efficiency in complex environment.

References

1. Brown, W.C.: Adapting microwave techniques to help solve future energy problems. In: 1973 IEEE G-MTT International Microwave Symposium, pp. 189–191 (1973)
2. Carver, K., Mink, J.: Microstrip antenna technology. Antennas and Propagation, IEEE Transactions on **29**(1), 2–24 (1981)
3. Fink, M.: Time reversal of ultrasonic fields. i. basic principles. Ultrasonics, Ferroelectrics, and Frequency Control, IEEE Transactions on **39**(5), 555–566 (1992)
4. Fink, M.: Time-reversal mirrors. Journal of Physics D: Applied Physics **26**(9), 1333 (1993)
5. Gavan, J., Tapuch, S.: Microwave wireless power transmission to highaltitude platform systems. Radio Science Bulletin (344), 25–42 (2010)
6. Ishimaru, A., Jaruwatanadilok, S., Kuga, Y.: Wireless communications through unknown obscuring media by using time-reversal technique. IEEE AP Communications (2005)
7. Ishimaru, A., Zhang, C., Stoneback, M., Kuga, Y.: Time-reversal imaging of objects near rough surfaces based on surface flattening transform. Waves in Random and Complex Media **23**(3), 306–317 (2013)
8. Jaruwatanadilok, S., Ishimaru, A., Kuga, Y.: Optimum wireless communication through unknown obscuring environments using the time-reversal principle: theory and experiments. In: Ultra-Wideband Short-Pulse Electromagnetics 8, pp. 105–112. Springer (2007)
9. Massa, A., Oliveri, G., Viani, F., Rocca, P.: Array designs for long-distance wireless power transmission: State-of-the-art and innovative solutions. Proceedings of The IEEE **101**(6), 1464–1480 (2013)
10. McSpadden, J.O., Mankins, J.C.: Space solar power programs and microwave wireless power transmission technology. Microwave Magazine, IEEE **3**(4), 46–57 (2002)
11. Nguyen, H.T., Andersen, J.B., Pedersen, G.F.: The potential use of time reversal techniques in multiple element antenna systems. IEEE Communications Letters **9**(1), 40–42 (2005)
12. Oda, Y., Yamaguchi, T., Komurasaki, K., Kajiwara, K., Takahashi, K., Sakamoto, K.: An experimental study on high power millimeter wave beam transmission for microwave beaming propulsion. In: Microwave Workshop Series on Innovative Wireless Power Transmission: Technologies, Systems, and Applications (IMWS), 2011 IEEE MTT-S International, pp. 181–184. IEEE (2011)

13. Oida, A., Nakashima, H., Miyasaka, J., Ohdoi, K., Matsumoto, H., Shinohara, N.: Development of a new type of electric off-road vehicle powered by microwaves transmitted through air. Journal of Terramechanics **44**(5), 329–338 (2007)
14. Oliveri, G., Poli, L., Massa, A.: Maximum efficiency beam synthesis of radiating planar arrays for wireless power transmission. Antennas and Propagation, IEEE Transactions on **61**(5), 2490–2499 (2013)
15. Oman, H.: Electric car progress. Aerospace and Electronic Systems Magazine, IEEE **17**(6), 30–35 (2002)
16. Orfanidis, S.J.: Electromagnetic waves and antennas. Rutgers University (2002)
17. Pozar, D.: Scattered and absorbed powers in receiving antennas. Antennas and Propagation Magazine, IEEE **46**(1), 144–145 (2004)
18. Prada, C., Manneville, S., Spoliansky, D., Fink, M.: Decomposition of the time reversal operator: Detection and selective focusing on two scatterers. The Journal of the Acoustical Society of America **99**, 2067 (1996)
19. Shams, K.M., Ali, M.: Wireless power transmission to a buried sensor in concrete. Sensors Journal, IEEE **7**(12), 1573–1577 (2007)
20. Shinohara, N.: Wireless power transfer via radiowaves. John Wiley & Sons (2014)
21. Vieira, J., Malkowsky, S., Nieman, K., Miers, Z., Kundargi, N., Liu, L., Wong, I., Owall, V., Edfors, O., Tufvesson, F.: A flexible 100-antenna testbed for massive mimo. In: Globecom Workshops (GC Wkshps), 2014, pp. 287–293. IEEE (2014)
22. Zhang, C., Ishimaru, A., Kuga, Y.: Time-reversal and music imaging of objects near rough surface based on surface flattening transform. In: Radio Science Meeting (USNC-URSI NRSM), 2013 US National Committee of URSI National. URSI (2013)
23. Zhao, D., Jin, Y., Wang, B.Z., Zang, R.: Time reversal based broadband synthesis method for arbitrarily structured beam-steering arrays. Antennas and Propagation, IEEE Transactions on **60**(1), 164–173 (2012)
24. Zhou, S., Giannakis, G.B.: Optimal transmitter eigen-beamforming and space-time block coding based on channel mean feedback. Signal Processing, IEEE Transactions on **50**(10), 2599–2613 (2002)